World Applied Sciences Journal 13 (6): 1295-1301, 2011
ISSN 1818-4952

Distortion-Free Embedding in the Optic Disk of Retina Fundus Images Using Complex-Valued Neural Network

R.F. Olanrewaju, O.O. Khalifa, Aisha- Abdulla, A.A. Aburas and A.M. Zeki

International Islamic University Malaysia (IIUM), P.O. Box: 10, 50728, Kuala Lumpur, Malaysia

Abstract: One of the downside of the current watermarking system is the inevitable distortion caused by data embedding. Some algorithms have been modified to produce a minimal distortion in the host image. However such small alterations may not be acceptable for medical images which are use for diagnosing and treatment of diseases. This paper presents a distortion-free method for embedding data in the optic nerves of retina images (fundus) accomplished by Complex-Valued Neural Networks. Features of the images are modeled in Fast Fourier Transform to obtain the complex values which serve as inputs to Complex-Valued Neural Network, (CVNN). The performance of the proposed technique has been evaluated using ROC graphs and Image Fidelity Measure (IFM). Results obtained indicate that the proposed algorithm can perfectly embed watermark in the host image without any distortion or loss of information which makes both host and the watermarked image perceptually indistinguishable. The novelty of the proposed algorithm is that it guarantees a complete recovery of the embedded data during watermark extraction provided the network is trained properly and correct weights are used. Hence it can improve correct diagnoses and therefore useful in authentication system.

Key words: Complex Backpropagation (CBP) · Complex Valued Feedfoward · Complex- Valued Neural Network (CVNN) · Fast Fourier Transform (FFT) · Digital Watermarking · Fundus Image

INTRODUCTION

Fundus image is the interior surface of the eye that include the optic nerves, macula and retinal blood vessels [1, 2]. This is as shown in Fig. 1. The optic nerve which is responsible for transmitting of electrical impulses from the retina to the brain is connected to the back of the eye near the macula has a visible portion of the optic nerve called the optic disc. Optic disk has been shown to provide diagnostic information related to diabetic retinopathy (DR) and glaucoma diseases. Such images are use for early detection of numbers of ocular diseases which still remain the legal cause of blindness in working age population [3]. Protection and authentication of such medical images are now becoming increasingly important in an e-health environment where images are readily distributed over electronic networks. Recently, Medical image watermarking has been applied to ensure patients information security [4], content verification [5] and medical image fidelity [6]. Although digital watermarking provide better data security, however, it is necessary to preserve the originality of information in the image to avoid performance loss for human (clinician) viewers, which is one of the main factors that can hinder proper diagnoses, treatment and thus misleading decision. Research has shown that current watermarking system introduces distortion, visual artifacts and loss of information during image manipulation, data embedding, bit replacement, quantization or truncation. Such distortion and loss of information in turns affect the quality of the watermarked image and medical ethics does not permit distortion nor lost of information in diagnosis images. Therefore a distortion free embedding is required for diagnostic surgery. Furthermore, various algorithms have been suggested for watermarking medical images [7-12]. However the effectiveness of each diagnosis from the watermarked image greatly depends on the quality of the acquired input image. Firstly, some of these algorithms embed information directly into the host image by addition of watermark bits or bit replacement in the host image, in doing so, distortion and visual artifacts arise in the watermarked image. On the other hand, some algorithms perform transformation on the host image in order to increase it robustness, which results into having phase and magnitude (real and imaginary part) of host image.

Corresponding Author: R.F. Olanrewaju, International Islamic University Malaysia (IIUM), P.O. Box: 10, 50728, Kuala Lumpur, Malaysia. Tel: 603-61964533. Fax: 603 6196 4463, E-mails: frashidah@yahoo.com & khalifa@iiu.edu.my.

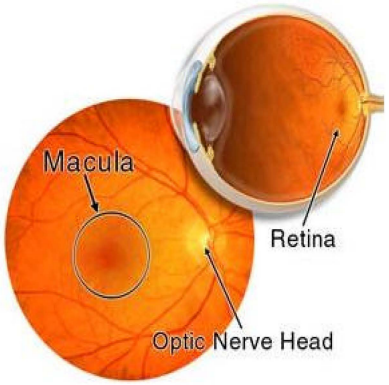

Fig. 1: Partial area of retina fundus image

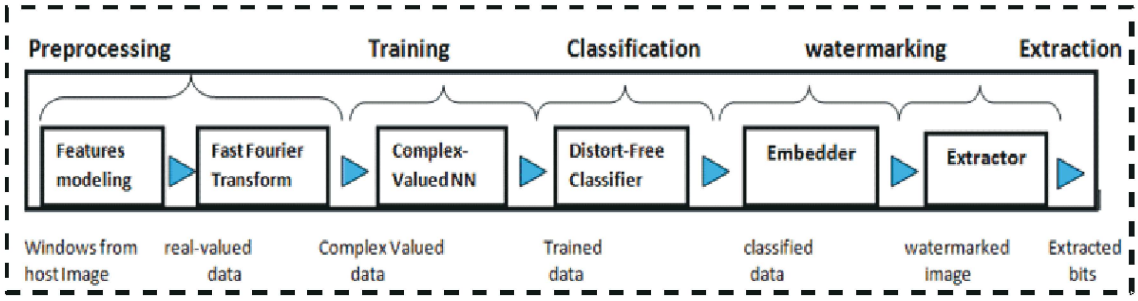

Fig. 2: Distortion-Free CVNN based watermarking system

Meanwhile, during embedding, only one component is considered, that is, either embedding in the phase or magnitude of the host image which leads to loss of information since using both real and imaginary components requires a complex embedding. Distortions caused due to loss of information, insertion/embedding in medical images is not accepted for diagnosis. With Distortion free embedding, it takes care of the distortion created during the watermarking process because the method involve mapping of watermark bits to the synapse weights of host image instead of direct embedding (adding) in the host image. This scheme also uses complex NN which help overcome loss of information by embedding in both components of host image (real and imaginary) accomplished by CVNN.

MATERIALS AND METHODS

Development of Distortion-Free CVNN-based Watermarking Model: The block diagram of the proposed Distortion-Free watermarking based CVNN (DFW-CVNN) is as shown in Fig. 2. It consists of a six stage cascade system, namely: Features modeling, Data FFT, CVNN, Distort-free classifier, Embedding and Extracting section.

Feature Modeling for DFW-CVNN: The global shape of retinal vessel structure shown in Fig. 1 is in general form. For better and precise location of region to embed the watermark, the whole image cannot be modeled by a single primitive form. Therefore, the nerve is segmented in small regions as in Fig. 3 in order to obtain the targeted windows by using block selector.

The block selection is based on the length of the watermark. Given a host image $I(m,n)$ watermark vector of length W_l and number of block to be selected bs the equation for total possible block that can be selected from $I(m,n)$ is defined as;

$$Tb_s = b_s \le W_l : \forall\, Tb_s \in I(m,n) \tag{1}$$

Fast Fourier Transform: Obtaining complex values from host image

The general model of obtaining complex values from. an image $I(x,y)$of size MXN using the fast version of Discrete Fourier Transform (DFT) is represented by $F(u,v)$

$$F(u,v) = \sum_{x=0}^{M-1}\sum_{y=0}^{N-1} I(x,y)e^{-j2\pi\left(\frac{ux}{M}+\frac{vy}{N}\right)} \tag{1}$$

for $x = 0, 1\ldots M-1, y = 0, 1\ldots N-1,$

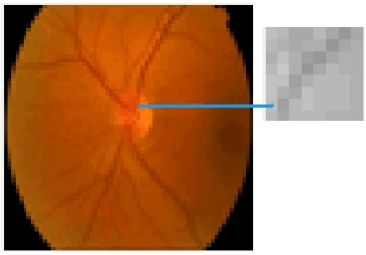

Fig. 3: Selected block from nerve end of Fundus image

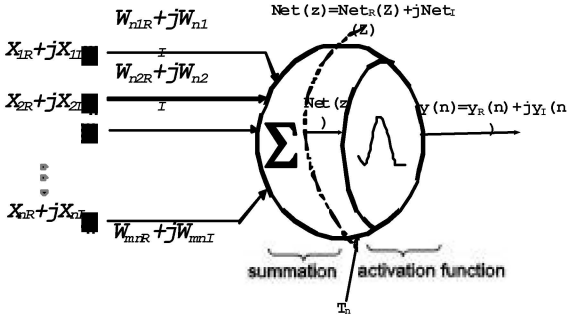

Fig. 4: Nonlinear adaptive complex neuron model

Thus given $F(u,v)$, $I(x,y)$ can be obtained back by means of the Inverse 2D DFT (2D IDFT);

$$I(x,y)=\frac{1}{MN}\sum_{x=0}^{M-1}\sum_{y=0}^{N-1}F(u,v)e^{j2\pi(\frac{ux}{M}+\frac{vy}{N})} \qquad (2)$$

Where u, v are frequency variables and x, y are spatial variables.

In this work, the FFT is applied on the host image so as to convert the spatial domain image to frequency domain in order to obtain the complex numbers. After selecting a block, before taking the FFT of each block, windowing function is applied. The windowing here is used to further enhance the ability of the FFT to extract spectral data from the host image.

Complex-Valued Neural Network Model: The model of complex value neuron used in this work is shown in Fig. 4, it is divided into two main part: the summation and the activation part.

It begins by summing up the weighted complex-valued inputs in order to obtain the threshold value which will be use to represent the internal state of a given input pattern. All the complex input are computed based on the complex algebra which results into a complex output through complex weights. The resultant sum is fed into the activation function which The CVNN is trained with Complex Backpropagation (CBP) [13, 14, 15]. This algorithm performs an approximation to the global minimization achieved by the method of steepest descent.

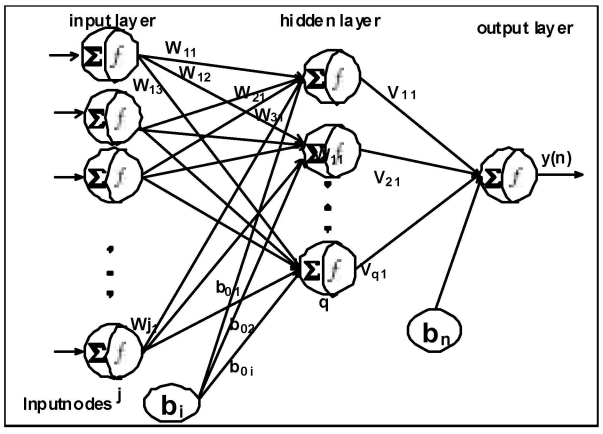

Fig. 5: Multilayer CVNN topology

For this study, CBP is applied to a multilayer CVNN, the architecture as shown in Figure 5. The sigmoid activation function used in this work is defined as:

$$Z=\frac{1}{1+exp^{-zR}}+j\frac{1}{1+exp^{-zI}} \qquad (3)$$

Where z_R and z_I are the real and imaginary threshold of the activation function respectively.

From the model neuron shown in 4, the net input/output relationship is characterized by nonlinear recursive equation given by:

$$Net_z=\sum_{1=1}^{j}X_jW_j1+b_i \qquad (4)$$

Where W_{jl} is the complex synaptic weight connecting complex-valued neuron j in input layer to hidden layer, X_j is the complex input signal from input layer, j is the no. of neuron in input layer and b_i is a bias value (complex-valued) of neuron i.

But

$$y(n)=\sum_{m=1}^{q}Net_zV_{q1}+b_n \qquad (5)$$

Where V_{ql} is the complex synaptic weight connecting complex-valued neuron q in hidden layer to output layer, Net_z is the output signal from complex hidden neuron.

The CVNN error to be propagated backward is defined as the difference between the desired response $d(n)$ and the actual output $y(n)$.

In it complex form, it becomes

$$e(n)=[d_R(n)+id_I(n)]-[y_R(n)+iy_I(n)] \qquad (6)$$

Where $[d_R(n)+id_I(n)]$ the desired complex is valued data and $[y_R(n)+iy_I(n)]$ is the output of the CVNN.

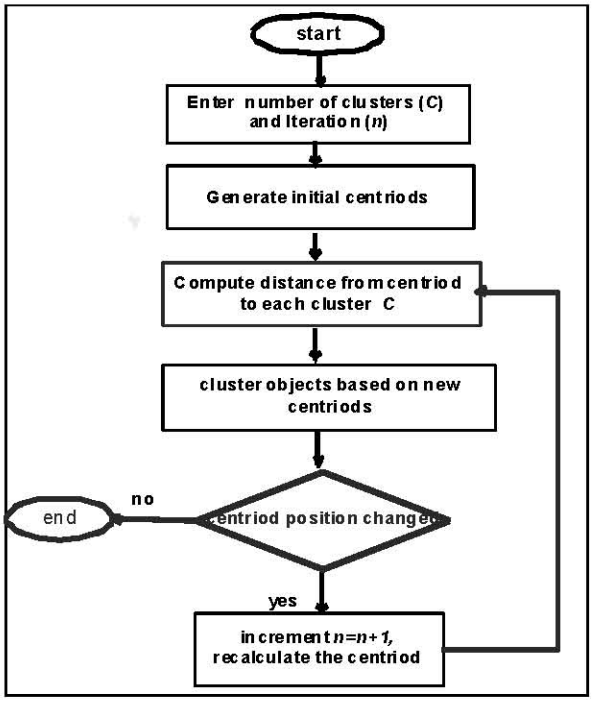

Fig. 6: Flowchart of Distortion-free classifier

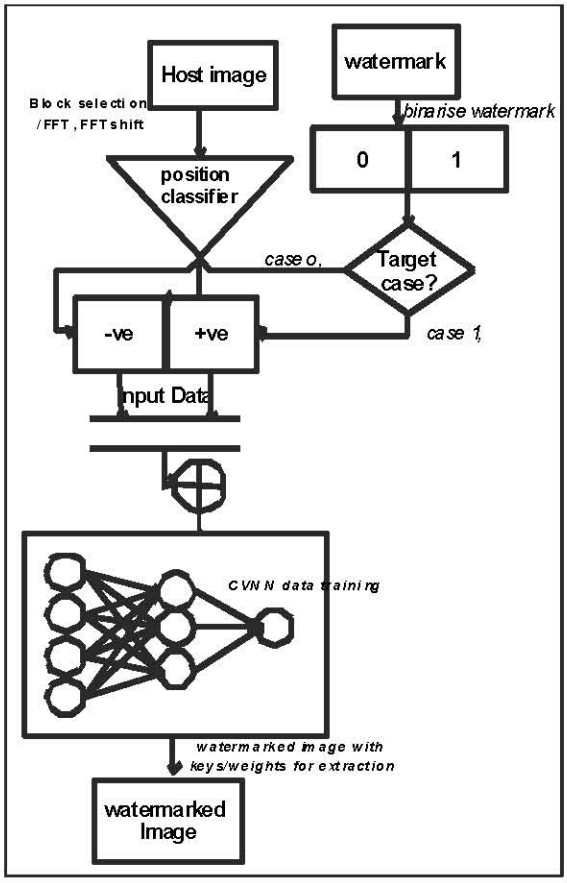

Fig. 7: Watermark embedding procedure

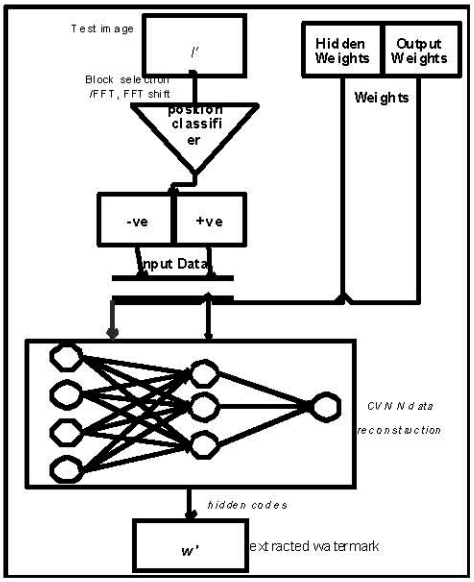

Fig. 8: Watermark extracting procedure

The CBP algorithm minimises the error function $e(n)$ by recursively adjust the weights and threshold values based on gradient search techniques.

Distortion Free Classifier: The main aim of the classifiers is to group the CVNN output into regions with same characteristics, that is either positive or negative. The classifier is used in partitioning into K group, [16, 17]. The algorithm finds the most optimum positioning of the K centers and then assigns each point to the most nearest center. The grouping is done by minimizing the sum of squares of distances between CVNN output and the corresponding cluster centroid. The algorithm flowchart is shown in Fig. 6.

Watermark Embedding Model: The main step in embedding is sufficient generation of weights (hidden and output) by the CVNN and carefully mapping of the target content (watermark bits) to the input data (host image). The embedding/mapping procedure is illustrated in Fig. 7.

Watermark Extraction Model: Watermark extraction is performed on a block-by-block basis for recovery of the hidden bits. During the training phase of CVNN, hidden nodes and output nodes weights are generated for each block. Those weights are saved for extraction. The block diagram for extraction procedure is shown in Fig. 8.

Extractor must receive correct position of each bit. Only by knowing the proper position of the bit will lead user to proper input values. This serves as a pointer to retrieving the proper network weights and only proper network weights will be able to output correct hidden bits.

The extractor then examines the extracted bits and compare with the values induced from the frequency component. The result of the hidden bits is threshold.

RESULTS AND DISCUSSION

The images used were obtained from fundus image DRIVE database [18]. The CVNN is configured with one hidden layer and the hidden neurons in the hidden layer varies from 4-5 nodes. After the FFT values of the host (fundus) image were calculated which contain real and imaginary components, these complex valued data were used as the input data to the CVNN. At the beginning of the training, weights and bias were initialize with small random complex values. After several experimentation, the optimum architecture nodes was found to be 11:5:1. The study was done in three phases; the output of the distortion-free classifier as shown in Table 1, the watermarked image as shown in Fig. 9 and the extraction of the watermark bit in Table 2.

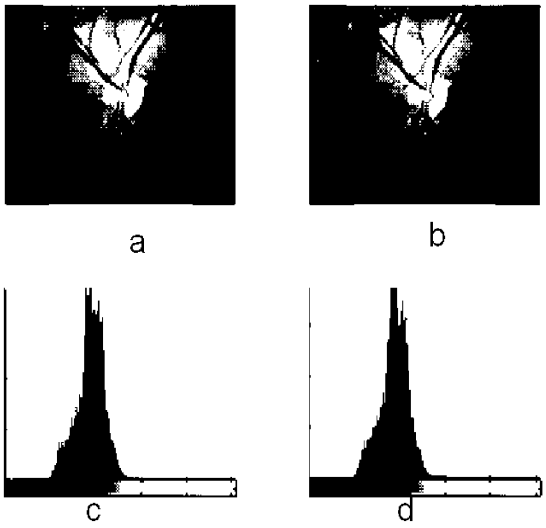

Fig. 9: Host image (a) watermarked (b), histogram of the image host(c) and histogram of watermarked fundus (d)

40% of the original values were use for training the network, after the network is converged; the next 40% were used as test data while the last 20% were used for validation. The host image 9(a), watermarked image 9(b), histogram of host 9(c) and watermarked image 9(d) is as shown in Fig. 9. From the histogram, both images are alike. In fact, the watermarked image is indistinguishable from the original host image. The watermarked image is highly imperceptible, that is the watermarked image and the host image are indistinguishable without any visual degradation. This is because of the watermarking strategy. In DFW-CVNN, no data was embedded directly into the host image, it rather uses a matching strategy to match the synapse weights of the host image to the watermark position, hence, there is no visual quality degradation to the watermarked image. It can be seen that both host and watermarked image are identical. Therefore, we concentrate on the accuracy of mapping strategy and watermark recovery. From Table 1, it can be seen that the CVNN has correctly classified the subjects by varying both the epoch (1500-3000)and the learning rate (LR) between 0.4-0.7. 100% mapping accuracy and precision rate is achieved. Also from the table the effect of numbers of neurons use in the hidden layer is observed. Using 5 neurons in hidden layer (HN), it shows that 100%

Table 1: Result of Distortion Free Classifier

HN	Epoch.	LR	P	N	TP	TN	FP	FN	ACC	PR	TPR	FPR
5	3000	0.7	1	2	1	2	0	0	1.00	1.00	1.00	1.00
5	3000	0.6	1	2	1	2	0	0	1.00	1.00	1.00	1.00
5	3000	0.5	1	2	1	2	0	0	1.00	1.00	1.00	1.00
5	3000	0.4	1	2	1	2	0	0	1.00	1.00	1.00	1.00
5	1500	0.7	1	2	1	2	0	0	1.00	1.00	1.00	1.00
5	1500	0.6	1	2	1	2	0	0	1.00	1.00	1.00	1.00
5	1500	0.5	1	2	1	2	0	0	1.00	1.00	1.00	1.00
5	1500	0.4	1	2	1	2	0	0	1.00	1.00	1.00	1.00
4	3000	0.7	1	2	1	2	0	0	1.00	1.00	1.00	1.00
4	3000	0.6	1	2	1	2	0	0	1.00	1.00	1.00	1.00
4	3000	0.5	1	2	1	2	0	0	1.00	1.00	1.00	1.00
4	3000	0.4	1	2	1	2	0	0	1.00	1.00	1.00	1.00
4	1500	0.7	1	2	1	2	0	0	1.00	1.00	1.00	1.00
4	1500	0.6	1	2	0	2	0	1	0.9	1.00	0.90	0.10
4	1500	0.5	1	2	1	2	0	0	1.00	1.00	1.00	1.00
4	1500	0.4	1	2	1	2	0	0	1.00	1.00	1.00	1.00

Table 2: Results of extracted watermark with correct hidden and output layer weights and quality measure of the extracted watermark

	Frequency components of recovered mark				Measure of Quality
Embedded watermark	Low	Mid	High	Recovered watermark, Thresholded	IFM
010	0.0553	0.9107	0.0443	010	0.9844
010	0.0049	0.9350	0.0465	010	0.9927
010	0.0005	0.9296	0.0608	010	0.9900
010	0.0491	0.8457	0.0875	010	0.9533
010	0.0096	0.9763	0.0266	010	0.9986
010	0.0378	0.9457	0.0424	010	0.9931
010	0.0201	0.9706	0.0238	010	0.9981
010	0.0205	0.9475	0.0582	010	0.9927
010	0.0289	0.9530	0.0304	010	0.9956
010	0.0027	0.9640	0.0436	010	0.9966
010	0.0366	0.9313	0.0560	010	0.9894
010	0.0002	0.9987	0.0104	010	0.9999
010	0.0000	0.9820	0.0327	010	0.9986
010	0.0001	0.9985	0.0162	010	0.9997
010	0.0030	0.9986	0.0374	010	0.9986
010	0.0312	0.9446	0.0084	010	0.9954
010	0.0706	0.8576	0.0502	010	0.9625
010	0.0284	0.9420	0.0223	010	0.9947
010	0.0460	0.9182	0.0207	010	0.9891
010	0.0484	0.8819	0.1029	010	0.9660

accuracy and precision was obtained for all the epoch and learning rate used. None of the instance is missed or mis-mapped. However for 4 hidden layer nodes, the watermark bits were mapped with 99% accuracy when learning rate 0.6 and 1500epoch were used. Other learning rates recorded 100% accuracy. This high percentage of classification results has a great effect on the watermark mapping strategy which in turn yielded a good result in retrieval of the watermark. If there were wrong classification, this will lead to mis-mapping of the watermark to the wrong frequency position, consequently, erroneous watermark will be retrieve for incorrect position. For the extracted watermark in Table 2, column 2-4 shows the frequency components of the extracted watermark. After threshold, the entire block with correct weights are correctly recovered. The recovered watermark bits (010) are equal to the mapped watermark bits (010). Column 6 of the table shows IFM between the embedded and the recovered watermarked. IFM value ranges between 0 - 1. When the result of two images is 1 it means they are similar while 0 means dissimilar, that is, higher value signifies closeness, it can be seen that all the values obtained for IFM are between 0.9999 and 0.9625 of 1.0000. This shows that CVNN helps in prevention of loss of information during embedding, hence during extraction, the watermark was correctly recovered with the correct weights.

CONCLUSION

This study suggests an efficient and distortion free digital watermarking algorithm using complex neural network and FFT. A mapping strategy is used in place of conventional embedding (+) structure, which has inherent advantage in terms of watermark extraction, distortion free of the host image requirements.

The major contribution of this work is the level of accuracy obtained by the classifier while the second contribution is the innovative application of CVNN in watermarking medical images to overcome the problem of distortion caused due to watermark insertion.

This work can further be use in demonstration of watermark forgery detection system since the extraction is based on the weights, hence the extracted weights can be use to determine if image is tampered or not.

REFERENCES

1. Poonkuntran, S., R.S. Rajesh and P. Eswaran, 2009. Imperceptible Watermarking Scheme for Fundus Images Using Intra-Plane Difference Expanding, International J. Computer and Electrical Engineering, 1(4): 1793-8163.

2. Yannuzzi, L., M. Ober, J. Slakter, R. Spaide, Y. Fisher, R. Flower and R. Rosen, 2004. Ophthalmic fundus imaging: today and beyond American J. Ophthalmol., 137(3): 511-524.
3. Li, H. and O. Chutatape, 2000. Fundus image Features extraction, Proceedings of the 22nd Annual International Conference of the IEEE Engineering in Medicine and Biology Society EMBS, 4: 3071-3073.
4. Ulutas, M., G. Ulutas and V.V. Nabiyev, 2010. Medical Image Security and EPR Hiding Using Shamir's Secret Sharing Scheme. J. Systems and Software, pp: 341-353.
5. Maeder, A., J. Dowling, A. Nguyen, E. Brunton and P. Nguyen, 2010. Assuring authenticity of digital mammograms by image watermarking. Digital Mammography, pp: 204-211.
6. Zain, J.M., A.R.M. Fauzi and A.A. Aziz, 2008. Clinical Evaluation of Watermarked Medical Images. IEEE int. Conf. on Engineering in Medicine and Biology Society, pp: 5459-5462.
7. Memon, N.A., S. Gilani and A. Ali, 2009. Watermarking of Chest CT Scan Medical Images for Content Authentication. IEEE Int. Conf. on Information and Communication Technologies, pp: 175-180.
8. Nayak, J., P. Subbanna Bhat, U.R. Acharya and M. Sathish Kumar, 2009. Efficient storage and transmission of digital fundus images with patient information using reversible watermarking technique and error control codes. J. Medical Systems, 33(3): 163-171.
9. Niranjan, U., 2004. Simultaneous storage of medical images in the spatial and frequency domain: A comparative study. Bio. Medical Engineering OnLine, 3: 17.
10. Trichili, H., M. Boublel, N. Derbel and L. Kamoun, 2003. A new medical image watermarking scheme for a better telediagnosis. Information And Communication Technologies, 1: 1498-1503.
11. Ulutas, M., G. Ulutas and V.V. Nabiyev, 2010. Medical Image Security and EPR Hiding Using Shamir's Secret Sharing Scheme. J. Systems and Software, pp: 341-353.
12. Wakatani, A., 2002. Digital watermarking for ROI medical images by using compressed signature image. Proc. of the 35th Annual Hawaii IEEE Int. Conf. on System Sciences, pp: 2043-2048.
13. Aibinu, A., M.J.E. Salami and A. Shafie, 2010. Determination of Complex Valued Parametric Model Coefficients Using Artificial Neural Network Technique, Advances in Artificial Neural Systems, pp: 1-11.
14. Kim, T. and T. Adali, 2002a. Complex Backpropagation Neural Network Using Elementary Transcendental Activation Functions. IEEE Proc. Acoustics, Speech and Signal Processing, 2: 1281-1284.
15. Faijul Amin, M. and K. Murase, 2009. Single-layered complex-valued neural network for real-valued classification problems. Neurocomputing, 72(4-6): 945-955.
16. Hartigan, J. and M. Wong, 1979. Algorithm AS 136: A K-means clustering algorithm. Applied Statistics, 28(1): 100-108.
17. Wang, H., J. Qi, W. Zheng and M. Wang, 2009. Balance K-Means Algorithm. Int. Conf. Computational Intelligence and Software Engineering, pp: 1-3.
18. Staal, J.J., M.D. Abramoff, M. Niemeijer, M.A. Viergever and B. Van Ginneken, 2004. Ridge based vessel segmentation in color images of the retina, IEEE Transactions on Medical Imaging, 23: 501-509.